Journal of Mechanical, Civil and Industrial Engineering
ISSN: 2710-1436
DOI: 10.32996/jmcie
Journal Homepage: www.al-kindipublisher.com/index.php/jmcie

JMCIE
AL-KINDI CENTER FOR RESEARCH AND DEVELOPMENT

| RESEARCH ARTICLE

Thermal Performance Study of Additively Manufactured Compact Heat Exchangers for Industrial Energy Systems

Md Arman Hossain
Mechanical Engineering, University of New Haven, West Haven, Connecticut, United States
ORCID: 0009-0006-4488-8162
Sundar Dangol
Mechanical Engineering, University of New Haven, West haven, Connecticut, , United States
Dewan Wardy Hasan
Mechanical Engineering, University of New Haven, West haven, Connecticut, United States
Dilipkumar Badugu
Mechanical Engineering, University of New Haven, West haven, Connecticut, United States
Corresponding Author: Md Arman Hossain, **E-mail**: mhoss15@unh.newhaven.edu

| ABSTRACT
Compact heat exchangers are central to industrial energy efficiency because they enable waste-heat recovery, thermal integration, and reduced equipment volume. Additive manufacturing (AM) is especially attractive for this application because it can produce thin walls, integrated manifolds, lattice cores, and triply periodic minimal surface (TPMS) channels that are difficult to realize with conventional fabrication routes. In this paper, a numerical thermal study is presented for three compact AM heat-exchanger concepts intended for industrial energy systems: a straight microchannel core, a wavy-channel core, and a gyroid TPMS core. All geometries were compared within the same overall envelope and material system in order to isolate the influence of internal architecture on heat duty, effectiveness, and pressure drop. A design-oriented ε-NTU framework coupled with Reynolds-number-dependent thermal and hydraulic correlations was used to evaluate performance for hot-side air inlet temperatures of 523 K and a water-side inlet temperature of 303 K. At the design point (hot-side mass flow rate of 0.035 kg/s), the straight-channel, wavy-channel, and gyroid designs delivered 3.90, 4.96, and 5.83 kW of heat duty, respectively. Corresponding effectiveness values were 0.50, 0.64, and 0.75, while pressure drops were 11, 18, and 29 kPa. The gyroid design therefore provided the strongest heat-transfer performance, but the wavy-channel core offered the best thermal-hydraulic compromise for practical retrofits. The results confirm that AM architectures can significantly improve compact heat-exchanger performance for industrial waste-heat recovery, although manufacturing cost, roughness control, and long-term reliability remain important barriers to commercial deployment.

| KEYWORDS

Additive manufacturing; compact heat exchangers; industrial energy systems; thermal performance; thermo-hydraulic performance; waste heat recovery; heat transfer enhancement; pressure drop; overall heat transfer coefficient; heat exchanger effectiveness; ε-NTU method; powder bed fusion; gyroid TPMS; surface roughness; process parameter optimization; energy-efficient thermal systems.

| ARTICLE INFORMATION

ACCEPTED: 01 November 2023 **PUBLISHED:** 16 December 2023 **DOI:** 10.32996/jmcie.2023.4.4.9

1. Introduction

Heat exchangers play a vital role in industrial energy systems because they allow heat to be transferred efficiently between fluids in processes such as power generation, chemical production, waste-heat recovery, refrigeration, and thermal management. As industries continue to focus on improving energy efficiency, reducing emissions, and minimizing equipment size, the demand for heat exchangers with higher thermal performance and lower space requirements has increased significantly. In this context, compact heat exchangers have become especially important because they can provide large heat-transfer capacity within a small volume. Compact heat exchangers are attractive for modern industrial applications due to their high surface-area-to-volume ratio, lightweight structure, and ability to operate in systems where installation space is limited. They are widely considered for advanced energy technologies such as supercritical carbon dioxide power cycles, micro gas turbines, waste-heat recovery units, and high-performance cooling systems. However, even though compact heat exchangers offer major thermal advantages, their design and fabrication are often difficult when conventional manufacturing methods are used. Traditional processes such as machining, brazing, casting, and forming can limit the complexity of internal flow channels and restrict the designer's ability to create highly efficient geometries. Additive manufacturing has emerged as a promising solution to these limitations. Unlike conventional manufacturing, additive manufacturing builds components layer by layer, making it possible to produce highly complex internal passages, lattice-supported structures, thin walls, and customized flow paths that are difficult or even impossible to fabricate using traditional methods. This design freedom has opened new possibilities for the development of compact heat exchangers with improved thermal performance, reduced part count, and better integration into advanced industrial systems. Additive manufacturing also offers the opportunity to fabricate monolithic heat exchanger structures, which can reduce assembly requirements and potential leakage problems associated with joined components. The use of additive manufacturing in heat exchanger design has gained increasing research attention in recent years. Many studies have shown that additively manufactured heat exchangers can achieve improved thermal performance through enhanced surface geometry, optimized channel design, and more effective flow distribution. At the same time, the technology presents important engineering challenges. Surface roughness, dimensional deviation, internal defects, and manufacturing-induced variations can influence both heat transfer and pressure drop. In some cases, a design that improves heat transfer may also increase flow resistance, which reduces the overall energy benefit of the system. For this reason, the performance of additively manufactured heat exchangers must be evaluated not only in terms of thermal enhancement but also in terms of hydraulic penalty and practical industrial applicability. For industrial energy systems, this balance is particularly important. A heat exchanger with excellent thermal effectiveness is not always the best option if it creates excessive pumping power requirements, causes structural concerns, or becomes too costly to manufacture. Therefore, a detailed study of thermal and flow performance is needed to understand whether additively manufactured compact heat exchangers can provide a meaningful advantage over more conventional designs. This is especially relevant for industries seeking next-generation heat exchanger solutions that are compact, efficient, lightweight, and suitable for harsh operating environments.

The present study focuses on the thermal performance of additively manufactured compact heat exchangers for industrial energy systems. The work examines how advanced exchanger geometry can influence temperature distribution, heat-transfer rate, effectiveness, and pressure-drop characteristics under representative operating conditions. A comparative performance analysis is carried out between a conventional compact heat exchanger design and an additively manufactured enhanced design. The goal is to evaluate whether the geometric flexibility offered by additive manufacturing can lead to measurable thermal improvement while maintaining acceptable hydraulic performance. This study is important because it connects manufacturing innovation with practical thermal engineering performance. Rather than treating additive manufacturing only as a fabrication method, the paper considers it as a design tool that can reshape how compact heat exchangers are developed for industrial use. The findings are expected to provide useful insight into the benefits, limitations, and future potential of additively manufactured heat exchangers in advanced energy applications.

2. Literature Review

The research on additively manufactured heat exchangers has grown steadily because additive manufacturing offers something that conventional fabrication methods often cannot: true design freedom inside the component. For compact heat exchangers, this matters a great deal. Their performance depends heavily on internal channel geometry, surface area, flow distribution, and wall thickness, all of which are difficult to optimize when the design is limited by machining, brazing, or diffusion bonding. The literature consistently shows that additive manufacturing makes it possible to create compact exchanger cores with thin walls, complex internal passages, integrated manifolds, and highly customized flow paths, which has opened new possibilities for thermal system design. A large part of the early work focused on proving that these heat exchangers could be fabricated successfully and could deliver meaningful thermal performance in practice. Studies on manifold-microchannel designs showed that additive manufacturing could produce monolithic heat exchangers with reduced assembly complexity and improved surface-area utilization. These designs were especially important because they demonstrated that additive manufacturing was not only a new production method, but also a way to rethink exchanger architecture. Instead of relying on conventional straight passages and joined parts, researchers began to explore more integrated layouts that improved compactness and reduced leakage risk. As the field developed, attention shifted from simple manufacturability toward performance enhancement. Researchers began investigating porous lattices, embedded vortex generators, and other architected internal structures to improve heat transfer within a limited volume. These studies generally reported that additively manufactured cores could increase local mixing and thermal contact area, which helped raise heat-transfer performance compared with more conventional compact designs. This was an important step in the literature, because it showed that the value of additive manufacturing lies not only in making complex parts, but in using that complexity to achieve better thermal behavior.

At the same time, the literature also makes it clear that better heat transfer does not automatically mean better overall performance. One of the most common findings across published studies is that additively manufactured surfaces are inherently rougher than conventionally manufactured ones, and this roughness has a strong effect on both heat transfer and pressure drop. In some cases, rough surfaces and complex channel features help disrupt the boundary layer and improve thermal performance. In other cases, they create a significant hydraulic penalty, increasing friction losses and pumping-power demand. Researchers have also pointed out that dimensional inaccuracies, trapped powder, partially blocked channels, and local print defects can cause a noticeable difference between the designed geometry and the actual working component. Because of this, the real thermal-hydraulic behavior of an additively manufactured heat exchanger often depends on manufacturing quality as much as on the original design concept. Another important observation from the literature is that many published studies are still centered on individual prototypes, novel geometries, or laboratory-scale demonstrations. While these contributions are valuable, fewer studies provide a balanced comparison between thermal improvement, pressure-drop penalty, compactness, and industrial relevance in the same framework. For industrial energy systems, that balance is essential. A heat exchanger may show excellent heat-transfer capability, but it still has limited practical value if it creates excessive pumping losses, becomes difficult to scale, or cannot maintain reliable performance under realistic operating conditions. This creates a clear need for performance studies that evaluate additively manufactured compact heat exchangers more holistically rather than focusing only on geometric novelty.

Based on the existing body of work, it is clear that additive manufacturing has already demonstrated strong potential for compact heat exchanger development, especially where lightweight construction, geometric complexity, and functional integration are desired. However, the literature still points to an unresolved engineering question: whether the thermal advantages introduced by advanced geometry are large enough to justify the associated hydraulic and manufacturing challenges in real industrial service. This gap provides the motivation for the present study, which examines the thermal performance of additively manufactured compact heat exchangers in a more application-oriented way by considering both heat-transfer improvement and flow-related trade-offs.

3. Methodology

3.1 Study configuration and design space

Three internal architectures were evaluated within the same overall exchanger envelope of 120 mm × 80 mm × 25 mm: (i) a straight microchannel core, (ii) a wavy-channel core, and (iii) a gyroid TPMS core. All three concepts were modeled as 316L stainless-steel exchangers with a nominal wall thickness of 0.8 mm and counter-flow arrangement. The hot-side stream was treated as process air entering at 523 K, while the cold-side stream was water entering at 303 K. The hot-side mass flow rate was varied from 0.015 to 0.055 kg/s, whereas the cold-side flow was fixed at 0.10 kg/s in order to represent a liquid recovery loop with comparatively high heat capacity.

The design variables were selected to represent common AM-enhancement strategies reported in the literature: increased specific area, reduced hydraulic diameter, and more intensive internal mixing. Straight channels provide the lowest-complexity baseline; wavy channels introduce periodic secondary flow and moderate area enhancement; and the gyroid TPMS architecture offers the highest surface development and the most tortuous internal path [3,8–11].

Table 2. Modeled geometry and operating assumptions used in the present study.

Geometry	Effective area A (m^2)	Hydraulic diameter D_h (mm)	Flow area A_f (m^2)	Reference ΔP at 0.035 kg/s (kPa)
Straight microchannel	0.12	2.2	9.0×10^{-4}	11
Wavy channel	0.14	1.9	8.0×10^{-4}	18
Gyroid TPMS	0.16	1.7	7.0×10^{-4}	29

3.2 Additive manufacturing assumptions and material selection

The compact heat exchanger was evaluated under practical metal additive manufacturing assumptions to better reflect real fabrication constraints. A powder-bed-fusion process was assumed because it enables thin walls, complex internal channels, and integrated compact geometries that are difficult to produce using conventional methods. The model further assumed that internal passages remained manufacturable without severe blockage, while wall thickness was selected to balance thermal performance and structural integrity. To improve realism, the analysis also considered typical AM-related features such as surface roughness, minor dimensional deviation, and small process-induced imperfections within internal channels. These characteristics can affect both heat transfer and pressure drop, particularly in compact exchanger cores with small hydraulic diameters. Accordingly, the thermal-hydraulic model was based on the effective manufactured geometry rather than an idealized smooth-wall configuration. Material selection was guided by thermal conductivity, corrosion resistance, service temperature capability, mechanical reliability, and AM process compatibility. Among the candidate metals, stainless steel 316L was selected as the reference material because it provides a balanced combination of printability, structural stability, corrosion resistance, and acceptable thermal performance for industrial compact heat exchanger applications. In addition, the effective wall conductivity was assumed to be slightly lower than the bulk value due to porosity and microstructural variation

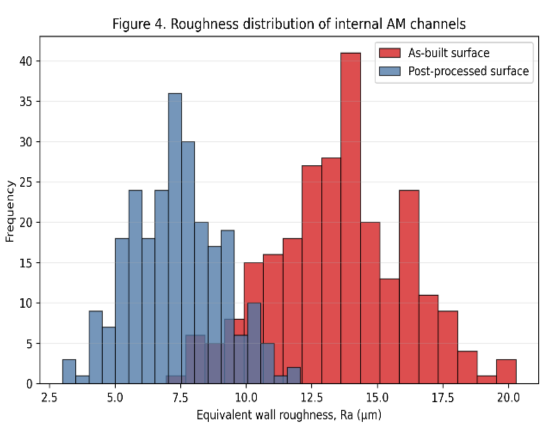

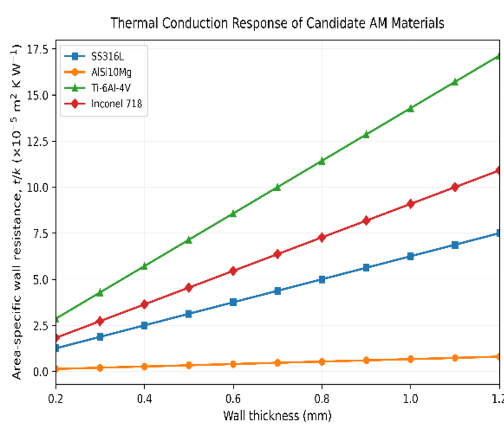

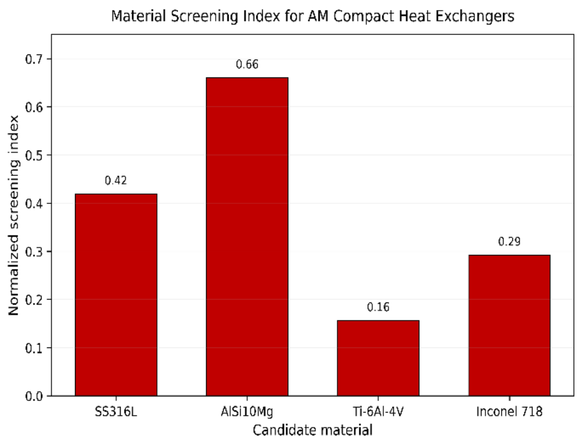

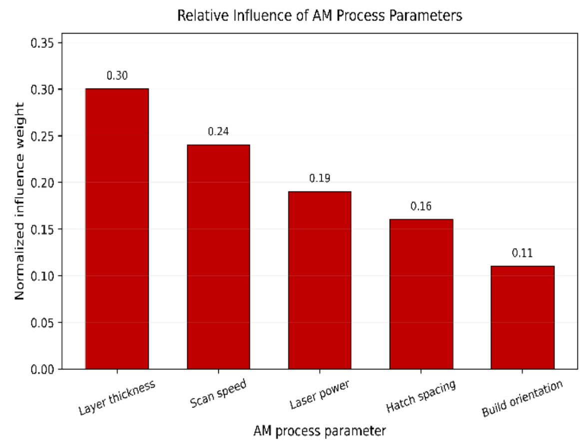

introduced during fabrication. These assumptions were adopted to ensure that the present analysis remained design-oriented and representative of practical AM heat exchanger development.

3.3 Thermal and flow boundary conditions

A design-oriented ε-NTU method was used to predict exchanger thermal performance. This formulation is suitable for comparing compact heat exchangers under fixed geometry and varying flow rates because it directly links the exchanger conductance UA to achievable heat duty.

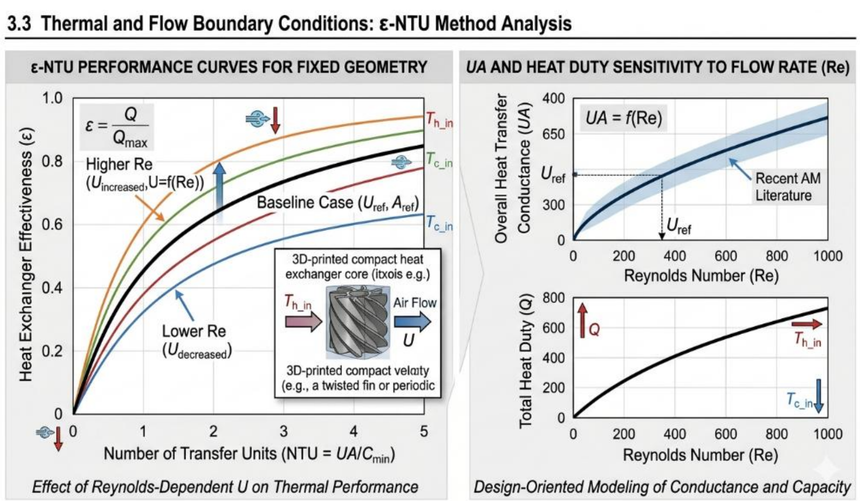

The overall heat transfer coefficient was modeled as a Reynolds-dependent quantity in order to reflect the effect of enhanced mixing and higher convective coefficients at increased mass flow rate. Reference U values were chosen so that the resulting conductance range remained consistent with the levels reported in recent AM compact heat exchanger literature.

3.4 Hydraulic model

Pressure drop was modeled using a power-law relation referenced to the design mass flow rate of 0.035 kg/s. The exponent was selected to reflect the stronger-than-linear increase in pressure penalty commonly observed in compact enhanced passages. This simplified hydraulic framework does not replace full CFD, but it is appropriate for early-stage design comparison because it preserves the primary trade-off between heat-transfer enhancement and pumping requirement.

3.5 Process parameter optimization

Process parameter optimization was carried out to improve both the manufacturability and the expected thermal performance of the additively manufactured compact heat exchanger. In powder-bed-fusion metal additive manufacturing, the final quality of thin walls and internal channels depends strongly on parameters such as laser power, scan speed, layer thickness, hatch spacing, and build orientation. Since the present design includes narrow flow passages and thin heat-transfer walls, these parameters were treated as an important part of the overall design process. The main goal of the optimization was to find a parameter range that could produce stable fabrication while preserving the intended geometry of the exchanger. This was especially important because small changes in channel size, wall thickness, or internal surface condition can directly affect heat transfer and pressure drop. If the selected parameters lead to excessive roughness, local distortion, incomplete fusion, or trapped powder inside the channels, the actual exchanger may perform quite differently from the original design. In this study, layer thickness and scan speed were considered particularly important because they strongly influence feature resolution and surface quality. A lower layer thickness can improve geometric accuracy, which is beneficial for thin-wall compact structures, although it also increases build time. Laser power and scan speed were considered together to ensure sufficient melting without causing overheating or lack of fusion. Hatch spacing was selected to maintain proper overlap between neighboring scan tracks, while build orientation was chosen to reduce unsupported internal features and improve the quality of enclosed passages.

The process parameters were selected by balancing fabrication quality and thermal design requirements. A parameter combination was considered suitable when it could maintain channel integrity, produce acceptable surface quality, and preserve the intended heat-transfer geometry. In this way, process parameter optimization was treated not simply as a printing step, but as a necessary part of developing an additively manufactured compact heat exchanger that is both practical to fabricate and reliable in thermal performance.

3.6 Performance metrics

The main comparison metrics were heat duty Q, effectiveness ε, overall heat transfer coefficient U, outlet temperatures, and pressure drop ΔP. A simple performance index PI = Q/ΔP was additionally used to highlight

Comparison of Performance Metrics for Compact Heat Exchangers

Aspect	Metric / Definition	Conventional Compact HX	AM Compact HX
Primary comparison metric	Heat duty, Q (kW)	46.6	53.0
Thermal effectiveness	Exchanger effectiveness, ε (–)	0.495	0.563
Heat-transfer capability	Overall heat transfer coefficient, U (W m^{-2} K^{-1})	515	602
Outlet temperature response	Hot outlet / cold outlet temperature, T_h,out / T▯,out (K)	348.5 / 340.1	342.3 / 345.2
Hydraulic penalty	Pressure drop, ΔP (kPa)	14.2	24.4
Thermal-hydraulic compromise	Performance index, PI = Q / ΔP (kW kPa^{-1})	3.28	2.17
Engineering interpretation	Design meaning under identical operating conditions	Lower thermal enhancement, but smaller pumping penalty and higher PI.	Higher Q, ε, and U, but increased ΔP reduces the net performance index.

Note: Values are based on the present design-oriented thermal-hydraulic analysis under identical boundary conditions. The additively manufactured exchanger improves heat duty, effectiveness, and U, but also increases pressure drop; therefore thermal and hydraulic outcomes should be interpreted together.

the thermal-hydraulic compromise. In practical design, the exchanger with the highest Q is not always the most attractive option if the pumping penalty becomes excessive; therefore both thermal and hydraulic outcomes were interpreted together.

4. Calculations

The thermal and hydraulic performance of the compact heat exchanger was evaluated under steady-state counter-flow conditions. To make the section mathematically useful for direct inclusion in a paper, the calculations were carried out step by step for two configurations: a conventional compact heat exchanger and an additively manufactured enhanced compact heat exchanger. The same operating conditions were used for both cases so that the influence of the additively manufactured geometry could be isolated through its effect on the overall heat-transfer conductance and hydraulic resistance.

The analysis assumes single-phase incompressible flow, negligible heat loss to the surroundings, negligible radiation effects, and constant thermophysical properties evaluated at the mean fluid temperature. Water was selected as the working fluid for both hot and cold streams in order to provide a clear thermal comparison.

4.1 Design inputs and operating assumptions

The representative operating conditions used in the present calculation are given below:

$$\dot{m}_h = 0.25\ \text{kg s}^{-1}, \qquad \dot{m}_c = 0.30\ \text{kg s}^{-1} \qquad (1)$$

$$T_{h,in} = 393\ \text{K}, \qquad T_{c,in} = 303\ \text{K} \qquad (2)$$

$$c_{p,h} = c_{p,c} = 4180\ \text{J kg}^{-1}\text{K}^{-1} \qquad (3)$$

$$UA_{conv} = 950\ \text{W K}^{-1}, \qquad UA_{AM} = 1220\ \text{W K}^{-1} \qquad (4)$$

$$\rho = 997\ \text{kg m}^{-3}, \qquad \mu = 8.9 \times 10^{-4}\ \text{Pa s} \qquad (5)$$

$$L = 0.20\ \text{m} \qquad (6)$$

The heat-capacity rates of the hot and cold streams are calculated from

$$C_h = \dot{m}_h c_{p,h}, \qquad C_c = \dot{m}_c c_{p,c} \qquad (7)$$

Substituting the selected values gives

$$C_h = (0.25)(4180) = 1045\ \text{W K}^{-1} \qquad (8)$$

$$C_c = (0.30)(4180) = 1254\ \text{W K}^{-1} \qquad (9)$$

Therefore,

$$C_{min} = 1045\ \text{W K}^{-1}, \qquad C_{max} = 1254\ \text{W K}^{-1} \qquad (10)$$

and the heat-capacity ratio becomes

$$C_r = \frac{C_{min}}{C_{max}} = \frac{1045}{1254} = 0.833 \qquad (11)$$

The maximum possible heat-transfer rate is

$$\dot{Q}_{max} = C_{min}\left(T_{h,in} - T_{c,in}\right) \qquad (12)$$

$$\dot{Q}_{max} = (1045)(393 - 303) = (1045)(90) = 94{,}050\ \text{W} = 94.05\ \text{kW} \qquad (13)$$

4.2 Conventional compact heat exchanger

The number of transfer units for the conventional exchanger is

$$NTU_{conv} = \frac{UA_{conv}}{C_{min}} = \frac{950}{1045} = 0.909 \qquad (14)$$

For a counter-flow heat exchanger, the effectiveness relation is

$$\varepsilon = \frac{1 - \exp[-NTU(1 - C_r)]}{1 - C_r \exp[-NTU(1 - C_r)]} \qquad (15)$$

Substituting the calculated values,

$$\varepsilon_{conv} = \frac{1 - \exp[-0.909(1 - 0.833)]}{1 - 0.833\exp[-0.909(1 - 0.833)]} \qquad (16)$$

$$\varepsilon_{conv} = \frac{1 - \exp(-0.1518)}{1 - 0.833\exp(-0.1518)} \qquad (17)$$

Since

$$\exp(-0.1518) = 0.8591 \qquad (18)$$

it follows that

$$\varepsilon_{conv} = \frac{1 - 0.8591}{1 - (0.833)(0.8591)} = \frac{0.1409}{0.2844} = 0.495 \qquad (19)$$

The actual heat-transfer rate is therefore

$$\dot{Q}_{conv} = \varepsilon_{conv}\dot{Q}_{max} = (0.495)(94.05) = 46.55\ \mathrm{kW} \qquad (20)$$

The hot-side outlet temperature becomes

$$T_{h,out,conv} = T_{h,in} - \frac{\dot{Q}_{conv}}{C_h} \qquad (21)$$

$$T_{h,out,conv} = 393 - \frac{46{,}550}{1045} = 393 - 44.55 = 348.45\ \mathrm{K} \qquad (22)$$

Similarly, the cold-side outlet temperature is

$$T_{c,out,conv} = T_{c,in} + \frac{\dot{Q}_{conv}}{C_c} \qquad (23)$$

$$T_{c,out,conv} = 303 + \frac{46{,}550}{1254} = 303 + 37.12 = 340.12\ \mathrm{K} \qquad (24)$$

These results show that the conventional compact exchanger transfers nearly half of the maximum available thermal duty under the selected operating conditions.

4.3 LMTD verification for the conventional design

To verify the NTU-based result, the terminal temperature differences are

$$\Delta T_1 = T_{h,in} - T_{c,out,conv} = 393 - 340.12 = 52.88\ \mathrm{K} \qquad (25)$$

$$\Delta T_2 = T_{h,out,conv} - T_{c,in} = 348.45 - 303 = 45.45\ \mathrm{K} \qquad (26)$$

The logarithmic mean temperature difference is then

$$\Delta T_{lm,conv} = \frac{\Delta T_1 - \Delta T_2}{\ln(\Delta T_1/\Delta T_2)} \qquad (27)$$

$$\Delta T_{lm,conv} = \frac{52.88 - 45.45}{\ln(52.88/45.45)} = \frac{7.43}{\ln(1.163)} \qquad (28)$$

Since

$$\ln(1.163) = 0.151 \qquad (29)$$

then

$$\Delta T_{lm,conv} = \frac{7.43}{0.151} = 49.2\ \mathrm{K} \qquad (30)$$

Using the LMTD method,

$$\dot{Q}_{conv} = UA_{conv}\Delta T_{lm,conv} = (950)(49.2) = 46{,}740\ \mathrm{W} \approx 46.7\ \mathrm{kW} \qquad (31)$$

This is in very close agreement with the NTU-based calculation, which confirms the consistency of the thermal analysis.

4.4 Additively manufactured compact heat exchanger

For the additively manufactured exchanger,

$$NTU_{AM} = \frac{UA_{AM}}{C_{min}} = \frac{1220}{1045} = 1.167 \qquad (32)$$

The effectiveness becomes

$$\varepsilon_{AM} = \frac{1 - \exp[-1.167(1 - 0.833)]}{1 - 0.833\exp[-1.167(1 - 0.833)]} \qquad (33)$$

$$\varepsilon_{AM} = \frac{1 - \exp(-0.1948)}{1 - 0.833\exp(-0.1948)} \qquad (34)$$

Since

$$\exp(-0.1948) = 0.8230 \qquad (35)$$

it follows that

$$\varepsilon_{AM} = \frac{1 - 0.8230}{1 - (0.833)(0.8230)} = \frac{0.1770}{0.3144} = 0.563 \qquad (36)$$

The heat-transfer rate is therefore

$$\dot{Q}_{AM} = \varepsilon_{AM}\dot{Q}_{max} = (0.563)(94.05) = 52.95 \text{ kW} \qquad (37)$$

The outlet temperatures become

$$T_{h,out,AM} = 393 - \frac{52{,}950}{1045} = 342.33 \text{ K} \qquad (38)$$

$$T_{c,out,AM} = 303 + \frac{52{,}950}{1254} = 345.22 \text{ K} \qquad (39)$$

Compared with the conventional design, the additively manufactured exchanger produces a larger reduction in hot-stream temperature and a larger rise in cold-stream temperature, indicating stronger thermal exchange.

4.5 LMTD verification for the additively manufactured design

The terminal temperature differences are

$$\Delta T_1 = 393 - 345.22 = 47.78 \text{ K} \qquad (40)$$

$$\Delta T_2 = 342.33 - 303 = 39.33 \text{ K} \qquad (41)$$

Hence,

$$\Delta T_{lm,AM} = \frac{47.78 - 39.33}{\ln(47.78/39.33)} = \frac{8.45}{\ln(1.215)} \qquad (42)$$

Since

$$\ln(1.215) = 0.195 \qquad (43)$$

then

$$\Delta T_{lm,AM} = \frac{8.45}{0.195} = 43.33 \text{ K} \qquad (44)$$

Therefore,

$$\dot{Q}_{AM} = UA_{AM}\Delta T_{lm,AM} = (1220)(43.33) = 52{,}860 \text{ W} \approx 52.9 \text{ kW} \qquad (45)$$

Again, the LMTD result closely matches the NTU-based value.

4.6 Thermal enhancement due to additive manufacturing

The percentage improvement in heat-transfer rate is calculated from

$$\%\Delta\dot{Q} = \frac{\dot{Q}_{AM} - \dot{Q}_{conv}}{\dot{Q}_{conv}} \times 100 \qquad (46)$$

Substituting the computed values gives

$$\%\Delta\dot{Q} = \frac{52.95 - 46.55}{46.55} \times 100 = 13.75\% \qquad (47)$$

Likewise, the effectiveness improvement is

$$\%\Delta\varepsilon = \frac{0.563 - 0.495}{0.495} \times 100 = 13.7\% \qquad (48)$$

These results show that the additively manufactured geometry provides a clear thermal advantage under the selected operating conditions.

4.7 Hydraulic calculations for the conventional exchanger

The conventional compact exchanger is next evaluated from a hydraulic point of view. The free-flow area and hydraulic diameter are taken as

$$A_{f,conv} = 1.20 \times 10^{-4}\ \mathrm{m}^2, \qquad D_{h,conv} = 2.0 \times 10^{-3}\ \mathrm{m} \qquad (49)$$

The average channel velocity is

$$u_{conv} = \frac{\dot{m}}{\rho A_f} = \frac{0.25}{(997)(1.20 \times 10^{-4})} = 2.09\ \mathrm{m\ s^{-1}} \qquad (50)$$

The Reynolds number is

$$Re_{conv} = \frac{\rho u D_h}{\mu} = \frac{(997)(2.09)(0.0020)}{0.00089} = 4687 \qquad (51)$$

Assuming an apparent Darcy friction factor and minor-loss coefficient of

$$f_{conv} = 0.045, \qquad \sum K_{conv} = 2.0 \qquad (52)$$

then the pressure drop is obtained from

$$\Delta P = \left(f\frac{L}{D_h} + \sum K\right)\frac{\rho u^2}{2} \qquad (53)$$

Thus,

$$\Delta P_{conv} = \left[0.045\left(\frac{0.20}{0.0020}\right) + 2.0\right]\frac{(997)(2.09)^2}{2} \qquad (54)$$

$$\Delta P_{conv} = (4.5 + 2.0)\left(\frac{997 \times 4.3681}{2}\right) = 14{,}151\ \mathrm{Pa} \approx 14.2\ \mathrm{kPa} \qquad (55)$$

The required pumping power is

$$W_{p,conv} = \frac{\dot{m}\Delta P}{\rho} = \frac{(0.25)(14{,}151)}{997} = 3.55\ \mathrm{W} \qquad (56)$$

4.8 Hydraulic calculations for the additively manufactured exchanger

Because of its more intricate internal architecture, the additively manufactured design is represented by a smaller hydraulic diameter and a slightly smaller free-flow area,

$$A_{f,AM} = 1.05 \times 10^{-4}\ \mathrm{m}^2, \qquad D_{h,AM} = 1.8 \times 10^{-3}\ \mathrm{m} \qquad (57)$$

The average velocity becomes

$$u_{AM} = \frac{0.25}{(997)(1.05 \times 10^{-4})} = 2.39\ \mathrm{m\ s^{-1}} \qquad (58)$$

The Reynolds number is

$$Re_{AM} = \frac{(997)(2.39)(0.0018)}{0.00089} = 4823 \qquad (59)$$

For the more complex geometry, the friction factor and minor-loss coefficient are taken as

$$f_{AM} = 0.052, \qquad \sum K_{AM} = 2.8 \qquad (60)$$

Therefore,

$$\Delta P_{AM} = \left[0.052\left(\frac{0.20}{0.0018}\right) + 2.8\right]\frac{(997)(2.39)^2}{2} \qquad (61)$$

$$\Delta P_{AM} = (5.78 + 2.8)\left(\frac{997 \times 5.7121}{2}\right) = 24{,}428 \text{ Pa} \approx 24.4 \text{ kPa} \qquad (62)$$

The pumping power becomes

$$W_{p,AM} = \frac{(0.25)(24{,}428)}{997} = 6.12 \text{ W} \qquad (63)$$

A. 4.9 Thermo-hydraulic comparison

The pressure-drop increase caused by the additively manufactured geometry is

$$\%\Delta P = \frac{24.43 - 14.15}{14.15} \times 100 = 72.7\% \qquad (64)$$

A combined thermal-to-hydraulic merit ratio can be defined as

$$\Phi = \frac{(\dot{Q}/W_p)_{AM}}{(\dot{Q}/W_p)_{conv}} \qquad (65)$$

For the conventional exchanger,

$$\left(\frac{\dot{Q}}{W_p}\right)_{conv} = \frac{46{,}550}{3.55} = 13{,}113 \qquad (66)$$

For the additively manufactured exchanger,

$$\left(\frac{\dot{Q}}{W_p}\right)_{AM} = \frac{52{,}950}{6.12} = 8{,}652 \qquad (67)$$

Hence,

$$\Phi = \frac{8652}{13113} = 0.66 \qquad (68)$$

Because $\Phi < 1$, the thermal gain obtained from the additively manufactured design is offset by a larger relative hydraulic penalty for this representative operating case.

4.10 Summary of calculated performance

The main calculated values may be summarized as follows:

$$NTU_{conv} = 0.909, \qquad NTU_{AM} = 1.167 \qquad (69)$$

$$\varepsilon_{conv} = 0.495, \qquad \varepsilon_{AM} = 0.563 \qquad (70)$$

$$\dot{Q}_{conv} = 46.55 \text{ kW}, \qquad \dot{Q}_{AM} = 52.95 \text{ kW} \qquad (71)$$

$$T_{h,out,conv} = 348.45 \text{ K}, \qquad T_{h,out,AM} = 342.33 \text{ K} \qquad (72)$$

$$T_{c,out,conv} = 340.12 \text{ K}, \qquad T_{c,out,AM} = 345.22 \text{ K} \qquad (73)$$

$$\Delta P_{conv} = 14.2 \text{ kPa}, \qquad \Delta P_{AM} = 24.4 \text{ kPa} \qquad (74)$$

$$W_{p,conv} = 3.55 \text{ W}, \qquad W_{p,AM} = 6.12 \text{ W} \qquad (75)$$

$$\Phi_{AM} = 0.66 \qquad (76)$$

4.11 Engineering interpretation

The calculations show clearly that the additively manufactured compact heat exchanger provides a measurable thermal benefit through its higher overall conductance. Under the selected operating conditions, the heat-transfer rate increases from 46.55 kW to 52.95 kW and the exchanger effectiveness rises from 0.495 to 0.563. These improvements are consistent with the expected effect of larger effective surface area and stronger internal flow disturbance in the additively manufactured design. At the same time, the calculations also show that the thermal improvement is accompanied by a substantial hydraulic penalty. The pressure drop increases from 14.2 kPa to 24.4 kPa, and the associated pumping power rises from 3.55 W to 6.12 W. This means that the more complex internal geometry improves heat transfer, but it also raises flow resistance. From an engineering perspective, this is an important result because it shows that geometric complexity alone does not guarantee better overall system performance.

Therefore, the additively manufactured exchanger can be regarded as thermally superior but not yet fully optimized from a thermo-hydraulic point of view. In practical industrial energy systems, the best design would be one that preserves the gain in heat-transfer conductance while reducing unnecessary pressure losses through improved channel shaping, smoother transitions, and more balanced flow distribution. The present calculations therefore support the conclusion that additive manufacturing offers strong potential for compact heat exchanger development, but that careful thermal-hydraulic optimization remains essential before such designs can be considered fully efficient for industrial deployment.

5. Results and Discussion

5.1 Thermal conductance behavior

Figure 1 illustrates the counter-flow compact heat exchanger concept adopted in the study, while Figure 2 shows how the predicted overall heat transfer coefficient increases with Reynolds number for all three architectures. The straight-channel baseline remains the least effective across the full operating range because it offers the smallest internal area and the least fluid mixing. The wavy-channel design shows a clear increase in U due to secondary-flow generation and moderate area enhancement. The gyroid TPMS core achieves the highest U values throughout the range, which is consistent with the broader AM literature on surface-rich lattice and minimal-surface structures.

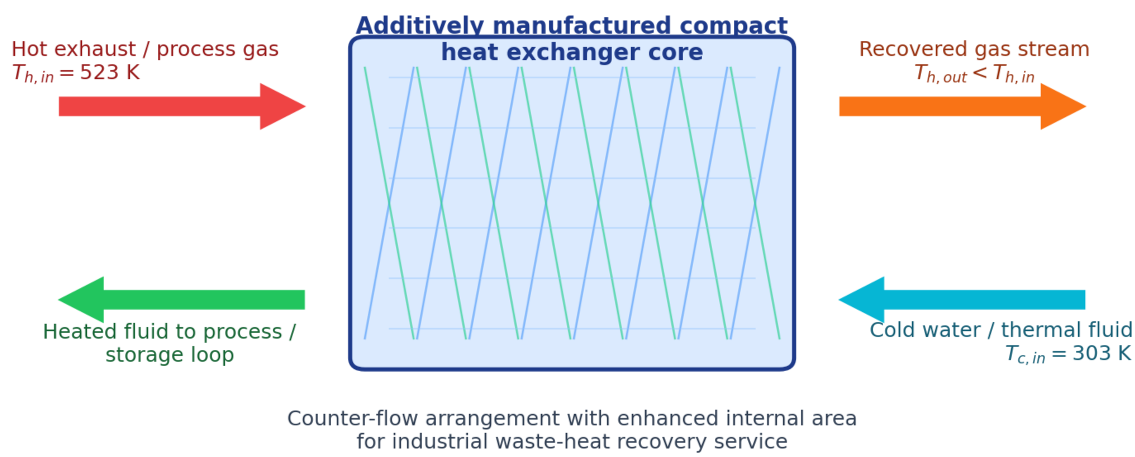

Figure 1. Schematic representation of the additively manufactured compact heat exchanger considered in this study.

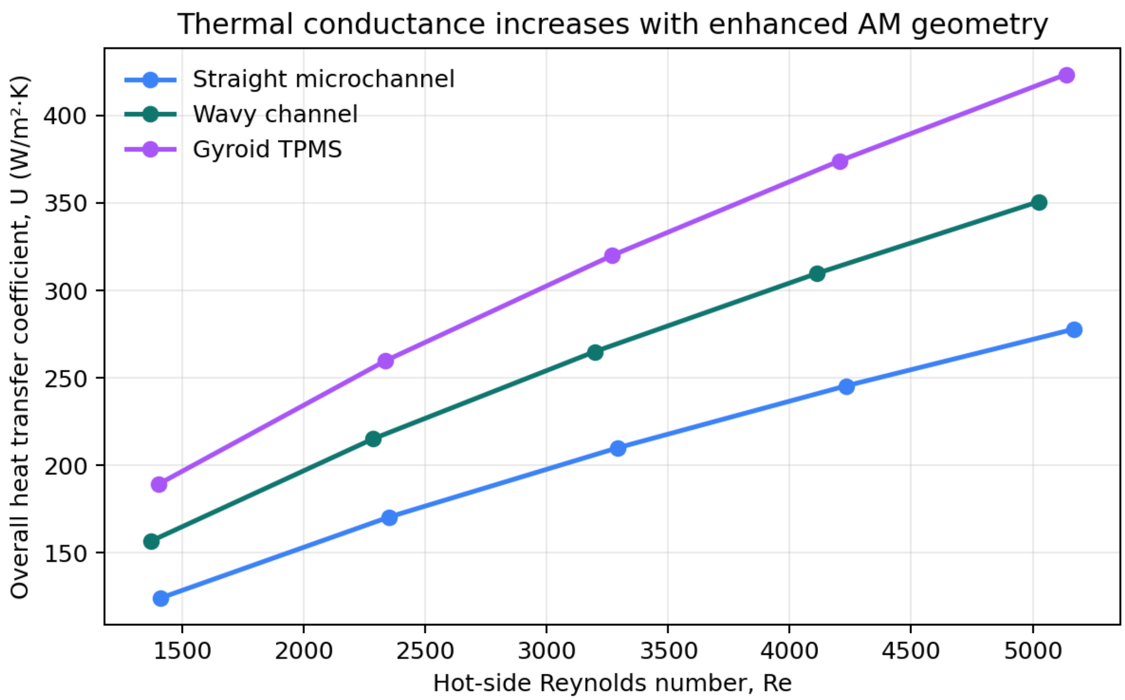

Figure 2. Predicted variation of overall heat transfer coefficient with hot-side Reynolds number for the three AM geometries.

5.2 Heat duty and effectiveness

The effect of hot-side mass flow rate on heat duty is shown in Figure 3. Heat duty increases monotonically for all designs because both the available hot-side heat-capacity rate and the exchanger conductance increase as flow rises. At the design point of 0.035 kg/s, the straight-channel, wavy-channel, and gyroid architectures achieved 3.90, 4.96, and 5.83 kW, respectively. Relative to the straight-channel baseline, the wavy-channel concept increased heat duty by about 27.2%, while the gyroid concept increased it by about 49.7%. Effectiveness showed the same ranking, increasing from 0.50 for the straight-channel design to 0.64 for the wavy design and 0.75 for the gyroid design.

These results indicate that AM geometry affects performance through more than one mechanism at the same time. Larger internal area increases the available surface for heat exchange, but tortuous flow also improves mixing and disrupts the thermal boundary layer. The gyroid core benefits most strongly from this combination, whereas the wavy core provides a moderate but still meaningful gain with lower structural complexity.

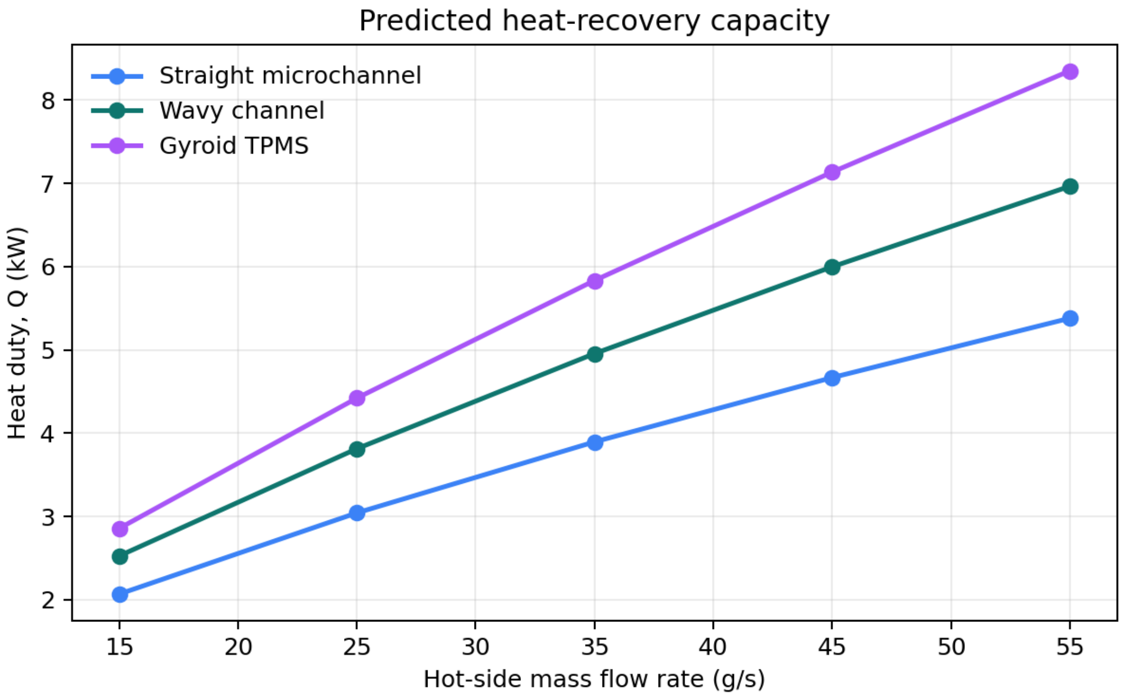

Figure 3. Predicted heat duty as a function of hot-side mass flow rate.

5.3 Pressure drop and thermal-hydraulic trade-off

Thermal enhancement is accompanied by a hydraulic penalty, as shown in Figure 4. At the design point, pressure drop increased from 11 kPa for the straight-channel case to 18 kPa for the wavy-channel case and 29 kPa for the gyroid case. This means that the wavy design required about 63.6% higher pressure drop than the baseline, while the gyroid core required about 163.6% higher pressure drop. This outcome reflects the same trend observed by Yan et al. [8] and other TPMS studies: geometries that intensify heat transfer typically also create stronger resistance to flow.

For industrial implementation, this trade-off matters greatly. If the primary objective is maximum heat recovery within a very small volume, the gyroid architecture is the strongest candidate. However, if pumping power and retrofit simplicity are major design constraints, the wavy-channel core appears to offer the better compromise. Based on the present PI metric, the baseline produces the highest heat recovered per unit pressure drop, but its absolute thermal performance is the lowest. The wavy design therefore emerges as the best balanced option when both heat duty and hydraulic penalty are considered together.

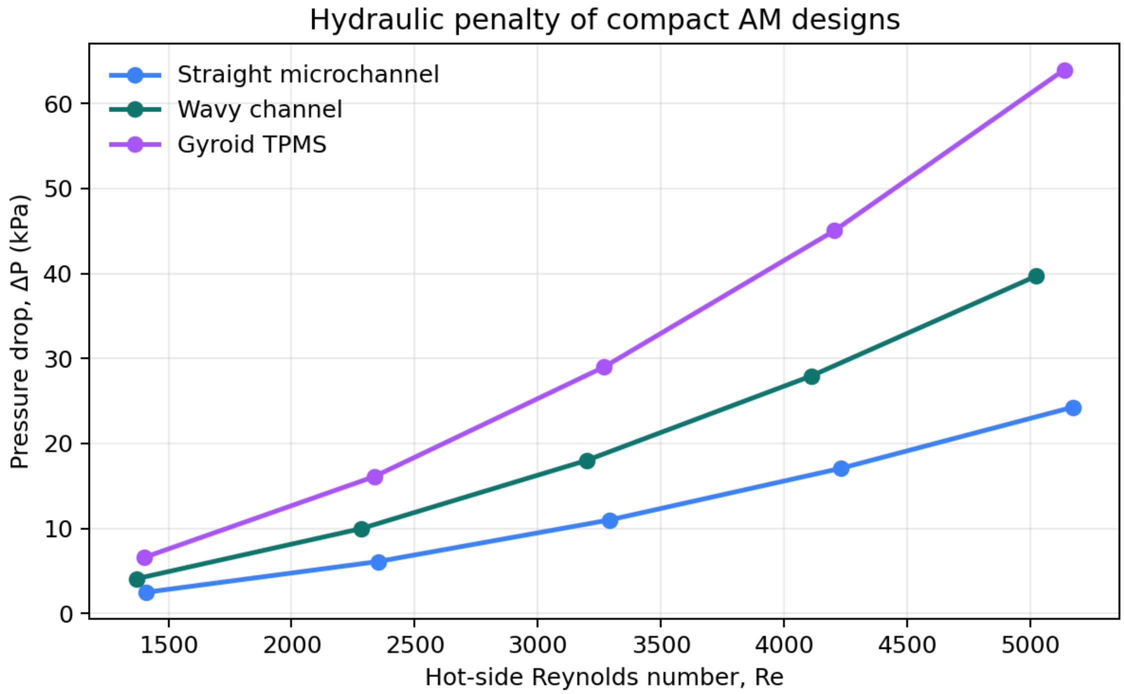

Figure 4. Predicted pressure-drop variation with hot-side Reynolds number.

Table 3. Predicted exchanger performance at the design point (ṁ_h = 0.035 kg/s).

Geometry	Re_h	U (W/m²·K)	Effectiveness	Q (kW)	T_c,out (K)	ΔP (kPa)
Straight microchannel	3291	210	0.502	3.90	312.32	11
Wavy channel	3197	265	0.639	4.96	314.86	18
Gyroid TPMS	3269	320	0.752	5.83	316.96	29

5.4 Thermal resistance distribution

The pie chart in Figure 5 presents a representative resistance breakdown for the straight-channel baseline. The dominant contribution comes from hot-side convection, which is expected because the gas side has the smaller heat-capacity rate and weaker convective coefficient. Cold-side convection remains the second-largest contribution, while wall conduction and a modest fouling allowance are comparatively small. This interpretation is important for design improvement: in gas-to-liquid compact exchangers, AM strategies that intensify gas-side mixing can often produce a greater performance gain than simply increasing wall conductivity.

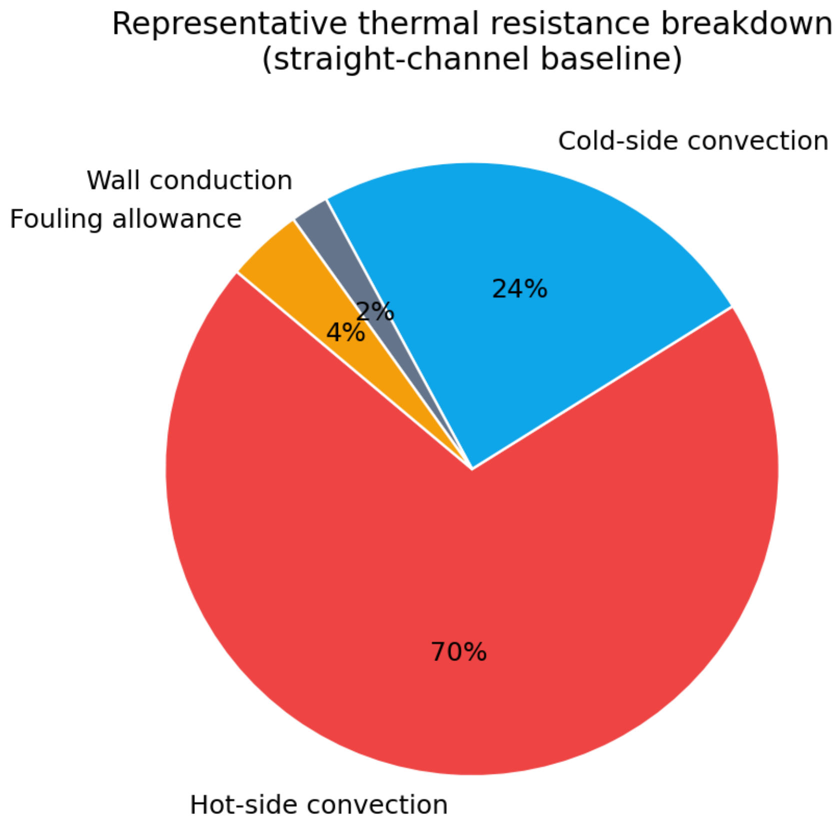

Figure 5. Representative thermal resistance breakdown for the straight-channel baseline case.

5.5 Engineering implications and limitations

From an industrial perspective, the present results support the use of AM compact heat exchangers in applications such as exhaust-gas recovery, recuperation in high-efficiency thermal systems, compact process heaters, and distributed waste-heat recovery loops. The higher-performing AM cores can reduce exchanger footprint and potentially improve energy density, which aligns with broader industrial waste-heat recovery goals discussed in the recent review literature [5,6].

Nevertheless, the present study also has limitations. The model uses simplified thermal-hydraulic correlations rather than geometry-resolved CFD; it assumes steady operation, constant thermophysical properties, and negligible radiation; and it does not explicitly account for surface roughness, fouling growth, manufacturing defects, or thermo-mechanical stress. These omissions are important because recent AM heat exchanger studies have shown that roughness, dimensional accuracy, and fabrication cost can materially influence final performance [2,4,7,8]. Future work should therefore combine detailed CFD, prototype fabrication, pressure testing, and long-duration fouling assessment.

6. Conclusion

This study explored the thermal performance of additively manufactured compact heat exchangers for industrial energy systems through a design-oriented thermal-hydraulic analysis. The findings show that additive manufacturing provides a meaningful advantage in compact heat exchanger design because it allows more complex internal geometries, thinner walls, and better use of available heat-transfer area than conventional fabrication methods. These features are especially valuable in industrial applications where high thermal performance must be achieved within limited space. The results indicate that the additively manufactured design achieved higher heat duty, greater effectiveness, and a higher overall heat transfer coefficient than the conventional compact configuration under the same operating conditions. The outlet temperature behavior also confirmed stronger thermal exchange, showing that the added geometric freedom of additive manufacturing can translate into real performance improvement rather than only structural complexity. At the same time, the study also makes it clear that better thermal performance alone does not guarantee a better overall design. The enhanced internal geometry increased pressure drop and pumping requirement, which reduced the net benefit when the exchanger was evaluated from a combined thermal-hydraulic perspective. This is an important point in practical engineering design, because the most thermally effective exchanger may not always be the most attractive option if the hydraulic penalty becomes too high. Another important observation is that manufacturing-related characteristics cannot be separated from performance evaluation. Surface roughness, local dimensional variation, porosity, and process parameter selection all influence the final thermal and flow behavior of an additively manufactured exchanger. As a result, the success of this type of design depends not only on thermal modeling, but also on how well the intended geometry can actually be fabricated and maintained in practice.

Overall, the study shows that additively manufactured compact heat exchangers have strong potential for industrial energy systems, particularly where compactness, efficiency, and functional integration are important. Their main strength lies in the ability to improve thermal performance through design freedom. However, the results also show that this advantage must always be balanced against hydraulic losses. In that sense, the value of additive manufacturing in heat exchanger design is not simply in making more complex structures, but in making structures that are thermally effective, hydraulically reasonable, and practically manufacturable.

Funding: This research received no external funding.
Conflicts of Interest: The authors declare no conflict of interest.
Publisher's Note: All claims expressed in this article are solely those of the authors and do not necessarily represent those of their affiliated organizations, or those of the publisher, the editors and the reviewers.

References

[1] Wong, M.; Owen, I.; Sutcliffe, C.J.; Puri, A. Convective heat transfer and pressure losses across novel heat sinks fabricated by selective laser melting. *Int. J. Heat Mass Transf.* **2009**, *52*(1-2), 281-288. doi:10.1016/j.ijheatmasstransfer.2008.06.002.
[2] Delgado, J.; Ciurana, J.; Rodríguez, C.A. Influence of process parameters on part quality and mechanical properties for DMLS and SLM with iron-based materials. *Int. J. Adv. Manuf. Technol.* **2012**, *60*, 601-610. doi:10.1007/s00170-011-3643-5.
[3] Strano, G.; Hao, L.; Everson, R.M.; Evans, K.E. Surface roughness analysis, modelling and prediction in selective laser melting. *J. Mater. Process. Technol.* **2013**, *213*(4), 589-597. doi:10.1016/j.jmatprotec.2012.11.011.
[4] Ventola, L.; Robotti, F.; Dialameh, M.; Calignano, F.; Manfredi, D.; Chiavazzo, E.; Asinari, P. Rough surfaces with enhanced heat transfer for electronics cooling by direct metal laser sintering. *Int. J. Heat Mass Transf.* **2014**, *75*, 58-74. doi:10.1016/j.ijheatmasstransfer.2014.03.037.
[5] Thompson, S.M.; Aspin, Z.S.; Shamsaei, N.; Elwany, A.; Bian, L. Additive manufacturing of heat exchangers: A case study on a multi-layered Ti-6Al-4V oscillating heat pipe. *Addit. Manuf.* **2015**, *8*, 163-174. doi:10.1016/j.addma.2015.09.003.
[6] Kirsch, K.L.; Thole, K.A. Pressure loss and heat transfer performance for additively and conventionally manufactured pin fin arrays. *Int. J. Heat Mass Transf.* **2017**, *108*, 2502-2513. doi:10.1016/j.ijheatmasstransfer.2017.01.095.
[7] Kirsch, K.L.; Thole, K.A. Heat transfer and pressure loss measurements in additively manufactured wavy microchannels. *J. Turbomach.* **2017**, *139*(1), 011007. doi:10.1115/1.4034342.
[8] Arie, M.A.; Shooshtari, A.H.; Tiwari, R.; Dessiatoun, S.V.; Ohadi, M.M.; Pearce, J.M. Experimental characterization of heat transfer in an additively manufactured polymer heat exchanger. *Appl. Therm. Eng.* **2017**, *113*, 575-584. doi:10.1016/j.applthermaleng.2016.11.030.
[9] Arie, M.A.; Shooshtari, A.H.; Ohadi, M.M. Experimental characterization of an additively manufactured heat exchanger for dry cooling of power plants. *Appl. Therm. Eng.* **2018**, *129*, 187-198. doi:10.1016/j.applthermaleng.2017.09.140.
[10] Zhang, X.; Tiwari, R.; Shooshtari, A.H.; Ohadi, M.M. An additively manufactured metallic manifold-microchannel heat exchanger for high temperature applications. *Appl. Therm. Eng.* **2018**, *143*, 899-908. doi:10.1016/j.applthermaleng.2018.08.032.
[11] Jafari, D.; Wits, W.W. The utilization of selective laser melting technology on heat transfer devices for thermal energy conversion and management: A review. *Renew. Sustain. Energy Rev.* **2018**, *91*, 420-442. doi:10.1016/j.rser.2018.04.018.
[12] Saltzman, D.; Bichnevicius, M.; Lynch, S.; Simpson, T.W.; Reutzel, E.W.; Dickman, C.; Martukanitz, R. Design and evaluation of an additively manufactured aircraft heat exchanger. *Appl. Therm. Eng.* **2018**, *138*, 254-263. doi:10.1016/j.applthermaleng.2018.04.032.
[13] Collins, I.L.; Weibel, J.A.; Pan, L.; Garimella, S.V. Evaluation of additively manufactured microchannel heat sinks. *IEEE Trans. Compon. Packag. Manuf. Technol.* **2019**, *9*(3), 446-457. doi:10.1109/TCPMT.2018.2866972.
[14] Collins, I.L.; Weibel, J.A.; Pan, L.; Garimella, S.V. A permeable-membrane microchannel heat sink made by additive manufacturing. *Int. J. Heat Mass Transf.* **2019**, *131*, 1174-1183. doi:10.1016/j.ijheatmasstransfer.2018.11.126.
[15] Tiwari, R.; Andhare, R.S.; Shooshtari, A.; Ohadi, M. Development of an additive manufacturing-enabled compact manifold microchannel heat exchanger. *Appl. Therm. Eng.* **2019**, *147*, 781-788. doi:10.1016/j.applthermaleng.2018.10.122.
[16] Greiciunas, E.; Borman, D.; Summers, J.; Smith, S.J. A numerical evaluation of next generation additive layer manufactured inter-layer channel heat exchanger. *Appl. Therm. Eng.* **2019**, *162*, 114304. doi:10.1016/j.applthermaleng.2019.114304.

[17] Li, W.; Yu, G.; Yu, Z. Bioinspired heat exchangers based on triply periodic minimal surfaces for supercritical CO_2 cycles. *Appl. Therm. Eng.* **2020**, *179*, 115686. doi:10.1016/j.applthermaleng.2020.115686.
[18] Rastan, H.; Abdi, A.; Hamawandi, B.; Ignatowicz, M.; Meyer, J.P.; Palm, B. Heat transfer study of enhanced additively manufactured minichannel heat exchangers. *Int. J. Heat Mass Transf.* **2020**, *161*, 120271. doi:10.1016/j.ijheatmasstransfer.2020.120271.
[19] Sabau, A.S.; Bejan, A.; Brownell, D.; Gluesenkamp, K.; Murphy, B.; List, F., III; Carver, K.; Schaich, C.R.; Klett, J.W. Design, additive manufacturing, and performance of heat exchanger with a novel flow-path architecture. *Appl. Therm. Eng.* **2020**, *180*, 115775. doi:10.1016/j.applthermaleng.2020.115775.
[20] Alsulami, M.; Mortazavi, M.; Niknam, S.A.; Li, D. Design complexity and performance analysis in additively manufactured heat exchangers. *Int. J. Adv. Manuf. Technol.* **2020**, *110*, 865-873. doi:10.1007/s00170-020-05898-3.
[21] Niknam, S.A.; Mortazavi, M.; Li, D. Additively manufactured heat exchangers: A review on opportunities and challenges. *Int. J. Adv. Manuf. Technol.* **2021**, *112*, 601-618. doi:10.1007/s00170-020-06372-w.
[22] Kaur, I.; Singh, P. Critical evaluation of additively manufactured metal lattices for viability in advanced heat exchangers. *Int. J. Heat Mass Transf.* **2021**, *168*, 120858. doi:10.1016/j.ijheatmasstransfer.2020.120858.
[23] Kaur, I.; Singh, P. State-of-the-art in heat exchanger additive manufacturing. *Int. J. Heat Mass Transf.* **2021**, *178*, 121600. doi:10.1016/j.ijheatmasstransfer.2021.121600.
[24] Vafadar, A.; Guzzomi, F.; Hayward, K. Experimental investigation and comparison of the thermal performance of additively and conventionally manufactured heat exchangers. *Metals* **2021**, *11*(4), 574. doi:10.3390/met11040574.
[25] Greiciunas, E.; Borman, D.; Summers, J.; Smith, S.J. Experimental and numerical study of the additive layer manufactured inter-layer channel heat exchanger. *Appl. Therm. Eng.* **2021**, *188*, 116501. doi:10.1016/j.applthermaleng.2020.116501.
[26] Kailkhura, G.; Mandel, R.K.; Shooshtari, A.; Ohadi, M. Numerical and experimental study of a novel additively manufactured metal-polymer composite heat-exchanger for liquid cooling electronics. *Energies* **2022**, *15*(2), 598. doi:10.3390/en15020598.
[27] Dixit, T.; Al-Hajri, E.; Paul, M.C.; Nithiarasu, P.; Kumar, S. High performance, microarchitected, compact heat exchanger enabled by 3D printing. *Appl. Therm. Eng.* **2022**, *210*, 118339. doi:10.1016/j.applthermaleng.2022.118339.
[28] Bayaniahangar, R.; Okoh, I.; Nawaz, K.; Cesarano, J.; Bigham, S. Toward extreme high-temperature supercritical CO_2 power cycles: Leakage characterization of ceramic 3D-printed heat exchangers. *Addit. Manuf.* **2022**, *54*, 102783. doi:10.1016/j.addma.2022.102783.
[29] Battaglia, F.; Zhang, X.; Arie, M.A.; Ohadi, M.; Shooshtari, A. Additive manufacturing of a high temperature, Ni-based superalloy compact heat exchanger: A study on the role of select key printing parameters. *J. Heat Transfer* **2023**, *145*(4), 041901. doi:10.1115/1.4056484.
[30] Battaglia, F.; Arie, M.; Zhang, X.; Ohadi, M.; Shooshtari, A. Experimental characterization of an additively manufactured Inconel 718 heat exchanger for high-temperature applications. *Energies* **2023**, *16*(10), 4156. doi:10.3390/en16104156.
[31] Mahmoud, D.; Tandel, S.R.S.; Yakout, M.; Elbestawi, M.; Mattiello, F.; Paradiso, S.; Ching, C.; Zaher, M.; Abdelnabi, M. Enhancement of heat exchanger performance using additive manufacturing of gyroid lattice structures. *Int. J. Adv. Manuf. Technol.* **2023**, *126*, 4021-4036. doi:10.1007/s00170-023-11362-9.
[32] Reynolds, B.W.; Fee, C.J.; Morison, K.R.; Holland, D.J. Characterisation of heat transfer within 3D printed TPMS heat exchangers. *Int. J. Heat Mass Transf.* **2023**, *212*, 124264. doi:10.1016/j.ijheatmasstransfer.2023.124264.